A Model and Measurement of Gravitational Waves Based on a Modified Yukawa Potential

Michael Harney [1]

[1]mharney1268@yahoo.com

Abstract: A model of gravitational waves is proposed using a complex Yukawa potential which is non-singular and predicts a dual-wave structure composed of incoming and outgoing waves. Using this potential, a fundamental gravitational wave frequency associated with the mass of the Universe is calculated to be the equal to Hubble's Constant. The characteristic out wave frequency of the Earth is calculated to be $3.38 \, x \, 10^{-5}$ Hz, which is in good agreement with the range of frequency of gravitation waves as predicted by Hawking and Israel. Also, the Lorentz transformation of the outgoing wave speed to the incoming wave speed predicts the same time dilation as the G44 solution from the Einstein field equations. Measurements with a high-resolution accelerometer sampled at 200 Hz over a period of 16, 24 and 32 hours demonstrates the signals with the expected frequencies of the Earth and Moon masses. These measurements show the Moon signal having a broader and more distinct peak during Full Moon and more diffuse during New Moon, consistent with the interaction of gravitational waves on the Sun side of the measurement, which diffuses the regular Moon signal to a lower level than the Full Moon.

I.   Introduction

The recent discovery of gravitational waves by LIGO has provided valuable confirmation of many predictions around gravitational waves. In particular, Hawking and Israel predicted gravitational waves would be observed in the frequency bands of 10^{-8} Hz to 10^{11} Hz [1]. The Laser Interferometer Space Antenna (eLISA) is a unique position to detect the lower end of this band at around 10^{-5} Hz, where it should be able to measure the signal of gravitational waves from the static potential due to the Earth and Moon. The European Pulsar Timing Array (EPTA) has high sensitivity in the 10^{-8} Hz range where it should be able to measure the static gravitational waves from the Sun. The following derivations of a non-singular Yukawa potential describes continuous gravitational waves that result from this static potential. The intermodulation of these continuous wave static wave sources, along with their associated motion, produces the modulated waves which are currently measured by LIGO and which will be measured in the future by eLISA and EPTA.

II.   A Complex Yukawa Potential

The standard, non-singular Yukawa potential is modeled by the following equation [2]:

$$V(r) = (A^2)\frac{e^{-kr}}{r}$$

(1)

Where A is the amplitude of the potential, k is a coupling constant associated with the particular force involved (in this case a gravitational constant that covers both the far field case of G and near field case of quantum gravity) and r is the range over which the potential acts, in this case the range is assumed to be from 0 to a limited distance encompassed within the Hubble sphere. We modify (1) to become a complex exponential:

$$V(r) = (A^2)\frac{e^{-kr}e^{i(\omega t + \emptyset)}}{r}$$

(2)

Where ω is the wave frequency and $\emptyset$ is the corresponding phase shift of the wave. In an environment where several of the waves in (2) travel towards a single point from all directions, with some asymmetry due to the slight variation of the mass density of local space, we theorize

a situation where the incoming waves meet at single point but also experience rotational asymmetry at a high-level. This would result in waves coming back in the same direction they originally came from, producing an interference pattern based on the changes in ω and $\emptyset$. With two potentials of this type oscillating in free space but moving in opposite directions with possibly a different frequency and different phase shifts, we arrive at the final potential:

$$V(r) = (A^2) \frac{e^{-kr}(e^{i(\omega_1 t + \emptyset_1)} - e^{i(\omega_2 t + \emptyset_2)})}{r}$$

(3)

III.   Properties of Interacting Yukawa Potentials

Figure 1 shows a graph of some possible interactions of standing wave potentials shows that the typical singularity of a particle potential (an electron in this case) associated with $1/r$ is replaced with a limiting value of A as r approaches zero due to the Yukawa potential. Figure 2 shows a similar situation where the wave potential has a negative amplitude (relative to the positive amplitude in Figure 1), resulting in the equivalent of a positron.
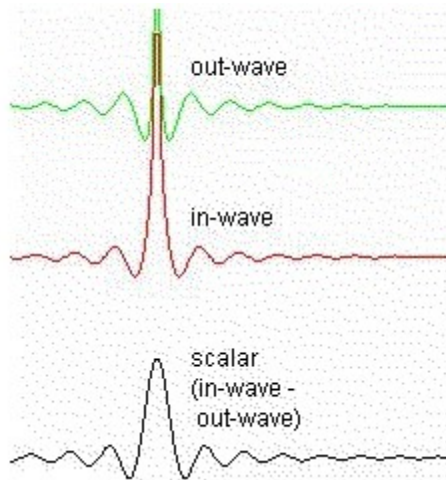
Figure 1. Interaction Between Potentials Moving in Opposite Directions – Electron
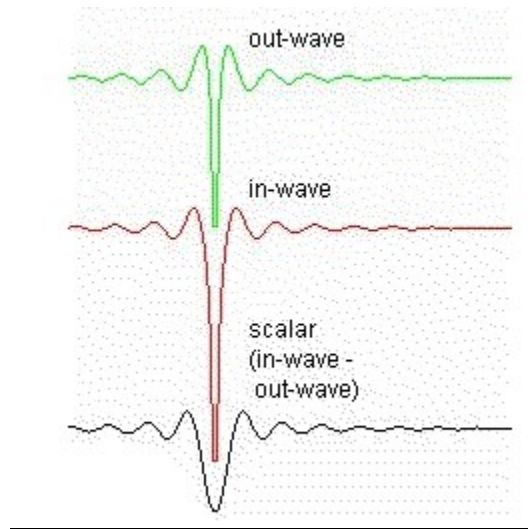
Figure 2. Interaction Between Potentials Moving in Opposite Directions with phase change – Positron

As discussed previously, in an environment where several of the waves in (2) travel towards a single point from all directions, there is the possibility of an asymmetry due to the slight variation of the mass density of local space, where the interacting wave center can experience rotational asymmetry (left-handed or right-handed rotation) which can be interpreted as spin of the particle. There is also the possibility of a phase shift between two wave centers which can correlate with the nature of charge (space tension due to wave centers that are out of phase). In the examples of Figure 1 and Figure 2, this would correspond to the wave centers between the electron and positron being out of phase by 180 degrees. Extensive characteristics of the spin and rotation associated with these interacting wave potentials has been evaluated previously by Wolf [3].

As the Yukawa potential in (2) has no dependency on the other spherical coordinates of φ or φ, the resulting scalar potentials of (2) and (3) can be interpreted as results of a scalar force equation of the form:

$$F(t) = m\ddot{r} + b\dot{r} + kr$$

(4)

Where m is considered a moving mass, b is considered the equivalent of a frictional coefficient, k is an elasticity constant of the corresponding wave medium and r is the range of interaction. If we identify particles of a standing wave nature as being permanent entities which is the

equivalent of $b = 0$, then for those transient particles that decay we infer that b is a non-zero value which controls the decay constant of b/m. Also, the frequency of the standing wave is controlled by the ratio of elasticity constant to the mass (k/m) with the frequency being determined from:

$$\omega = \sqrt{\frac{k}{m}}$$

(5)

The rotational effects of the wave center also changes the speed of the out-going waves based on distance r from the wave center:

$$v = \omega r$$

(6)

IV.   Gravitational Effects of Multiple Wave Centers

To determine k for gravitational effects, we look at the results of potential energy equivalence to moving mass density,

$$\frac{1}{2}kr^2 = \frac{1}{2}mv^2$$

(7)

From a previous determination of the wave velocity v as the speed of light and knowing there are two interacting waves [4] we arrive at,

$$\frac{1}{2}kr^2 = mc^2$$

(8)

We can determine k from (8) for gravitational effects for approximate values of the mass of the universe (m = 5.4 x 10^{52} Kg) and its radius ($r = 1.9$ x 10^{26} meters) [5],

$$k = \frac{2mc^2}{r^2} = 2.7 \text{ x } 10^{17} \text{ Newtons/meter}$$

(9)

Then for waves that are traveling across the Hubble radius of the universe, ω in (5) for the mass of the Universe becomes,

$$\omega = \sqrt{\frac{k}{m}} = \sqrt{\frac{2.7 \text{ x } 10^{17}}{5.4 \text{ x } 10^{52}}} = 2.23 \text{ x } 10^{-18} \frac{radians}{sec} = Hubble's\ Constant$$

(10)

The results of (10) shows that the fundamental node of standing wave frequencies in this universal model is the Hubble frequency, which is the in-coming wave for all matter in the Universe. Using this model, the cosmological redshift can be explained by understanding the energy transfer through incoming waves and how we view that energy as a function of distance, removing the need for a Doppler shift due to universal expansion [6].

To determine the out-going wave frequency of an object, we need to consider the local mass density around that object. The in-coming waves converge on a local mass density and are rotated and reflected back at a frequency based on local mass density. The results of (7) – (10) can be applied at individual wave level but are demonstrated here by aggregating wave affects to a macroscopic level, with many wave centers combining to produce the gravitational effects that we measure.

For the mass of the Earth, M_E = 5.972 x 10^{24} Kg we find the characteristic ω as,

$$\omega = \sqrt{\frac{k}{m}} = \sqrt{\frac{2.7 \text{ x } 10^{17}}{5.97 \text{ x } 10^{24}}} = 2.13 \text{ x } 10^{-4} \frac{radians}{sec} = 3.38 \text{ x } 10^{-5}\ Hz$$

(11)

For the mass of the Sun, M_S = 2.0 x 10^{30} Kg we find the characteristic ω as,

$$\omega = \sqrt{\frac{k}{m}} = \sqrt{\frac{2.7 \text{ x } 10^{17}}{2.0 \text{ x } 10^{30}}} = 3.67 \text{ x } 10^{-7} \frac{radians}{sec} = 5.85 \text{ x } 10^{-8}\ Hz$$

(12)

For the mass of the Moon, $M_M = 7.34 \times 10^{22}$ Kg we find the characteristic ω as,

$$\omega = \sqrt{\frac{k}{m}} = \sqrt{\frac{2.7 \times 10^{17}}{7.34 \times 10^{22}}} = 1.92 \times 10^{-3} \frac{radians}{sec} = 3.05 \times 10^{-4} \; Hz$$

(13)

As the wave energy falls off as *1/r* and the amplitude-squared (A^2) of the wave is proportional to the rest-energy of the object, we can expect similar results of gravitational influence by applying the traditional gravitational potential of *GM/r* to determine the effect from a given distance.

It is interesting to note that (6) shows the out wave speed from a mass is proportional to frequency and distance ($v = \omega r$). From a given out-wave speed we can also determine a time dilation relative to the in-wave speed (which is the speed of light for most cases) through the Lorentz transformation of the out-wave velocities relative to the in-wave velocities:

$$T = \frac{T_0}{\sqrt{1 - \frac{(\omega r)^2}{c^2}}} = \frac{T_0}{\sqrt{1 - \frac{v^2}{c^2}}}$$

(14)

If we use the Earth as an example, $\omega = 2.13 \times 10^{-4}$ and at distance from the center of the Earth of *r* = 26,000 km (GPS orbit) we find that the time dilation from (14) is:

$$T = \frac{T_0}{\sqrt{1 - \frac{(2.13 \times 10^{-4} \; x \; 26 \times 10^6)^2}{c^2}}} = 1.0000000001703 = \mathbf{170.3 \; psec \; change}$$

(15)

Performing the same calculation with General Relativity G44 solution (assuming a non-rotating sphere) gives the same result:
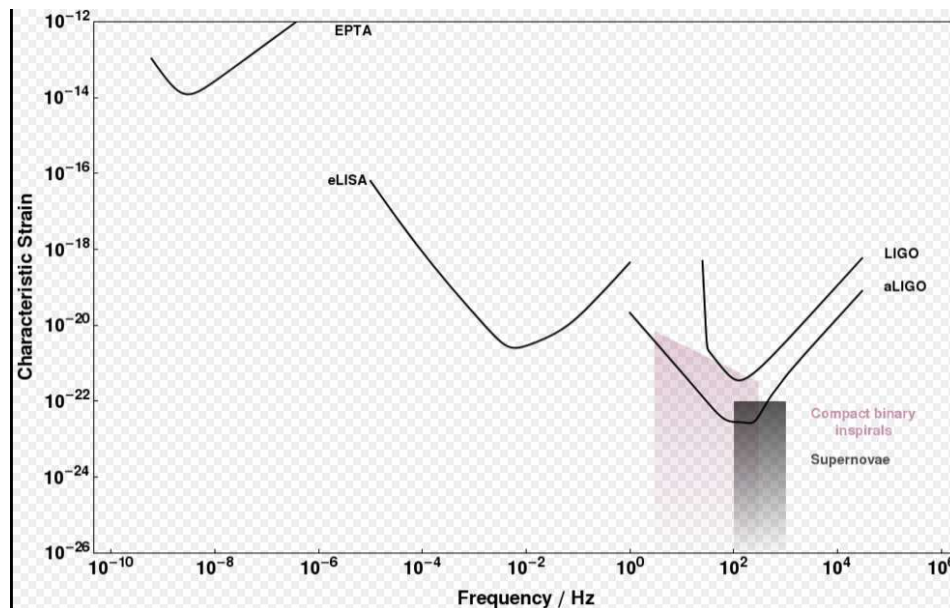
$$T = \frac{T_0}{\sqrt{1 - \frac{2GM}{rc^2}}} = \frac{T_0}{\sqrt{1 - \frac{2*(6.67 \; x10^{-11})(5.97 \; x10^{24})}{(26 \; x \; 10^6)c^2}}} = 1.0000000001703$$
$$= \mathbf{170.3 \; psec \; change}$$

(16)

V.   Measurement with LIGO-Based Platforms

The platforms currently in use or in development that has the potential to directly measure static gravitational waves or the result of up-modulation between two static wave sources (such as in binary black-hole mergers) (Figure 3).

Figure 3. Gravity Wave Detectors in Use or Planned for Future Use

From Figure 3, it is most likely going to be the Evolved Laser Interferometer Space Antenna (eLISA) which sees the monthly variation in the static gravitational wave source between the Earth and Moon (both out wave frequencies fall within the 10^{-5} Hz to 10^{-3} Hz range) when it is fully implemented [7]. The low-frequency static waves from the Earth and Moon are likely to present as a low-noise background with an orbital variation based on the satellite position with respect to the Earth-Moon orbit. The static out wave signal of $9.54x\ 10^{-8}\ Hz$ from the Sun would be measurable with the orbital variation of the European Pulsar Timing Array (EPTA).

VI.   Measurement Of Earth/Moon Signals with Accelerometer

An experiment was performed with a sensitive accelerometer that is capable of measuring the Earth and Moon's gravitational field. The potential of the Earth's gravity at a latitude of approximately 40.76 degrees (R_E estimated to be 6365 Km):

$$\frac{GM_E}{R_E} = 62{,}581{,}681\,\frac{J}{Kg}$$

(17)

The Moon's gravity at surface of the Earth (approximate based on latitude and using a mean between apogee and perigee of R_{ME} = 380,000 Km) is:

$$\frac{GM_M}{R_{ME}} = 12{,}883\,\frac{J}{Kg}$$

(18)

The ratio of the signal measured from the Moon relative to the signal measured from the Earth (with the measurement taken on the surface of the Earth as in (17)) is:

$$\frac{12{,}883}{62{,}581{,}681} = 2.06\ x\ 10^{-4}$$

(19)

This analysis is performed using Newtonian concepts that aggregate over all gravitational wave frequencies and does not take into account the frequency analysis of the Moon and Earth calculated in (11), (12) and (13), although we would expect the majority of the force components to exist at these frequencies. Also, the frequencies calculated in (11), (12) and (13) are what we would expect in the far field at multiples radii of these objects however, in the near field of measurement (such as our measurement on the Earth), we would expect some high-frequency energy to make up the force we measure as these high-frequency signals have yet to coalesce into the far-field signal. Therefore, we would expect the signal measured from the Moon relative to the signal measured from the Earth (with the measurement taken on the surface of the Earth) as shown in (19) to be much closer to unity as the signal of the Earth measured on the surface of the Earth will be near-field and have a wider distribution of energy across the frequency band, with less energy at the Earth's characteristic frequency. The signal of the Moon as measured on the surface of the Earth is easily considered far field as its radius is 1.73 million meters and it's mean distance from the Earth is 380 million meters (Distance$_{Moon-Earth}$ / Radius$_{Moon}$ = 219). Therefore, we would expect a normalized, far-field gravitational measurement of the Moon at its characteristic frequency when measured from the surface of the Earth, but a weaker than expected signal at the characteristic frequency from the Earth due to the near-field frequency spread.

To measure the Moon and Earth signals at the frequencies calculated in (11) and (13), we developed a fixture that is vibrationally-damped across low-frequencies and mounted a high-resolution MEMs accelerometer board to this fixture. The MEMS accelerometer used in the experiment is a Murata SCA610-E23H1A-1 with a 1.5 g range, 5V DC supply and a sensitivity of 1.33V/g. The sensor was connected as per data sheet recommendations. The sensor is mounted to a PCB and a mounting structure that reduces vibrational impact on the measurement as shown in Fig. 4. We excluded the Sun's characteristic frequency from our current measurements as the time resolution calculated to see the Sun's characteristic signal would require a continuous measurement time of approximately 3 years, but we do believe that a wider-band signal from the Sun does influence the following measurements of the Earth and Moon.
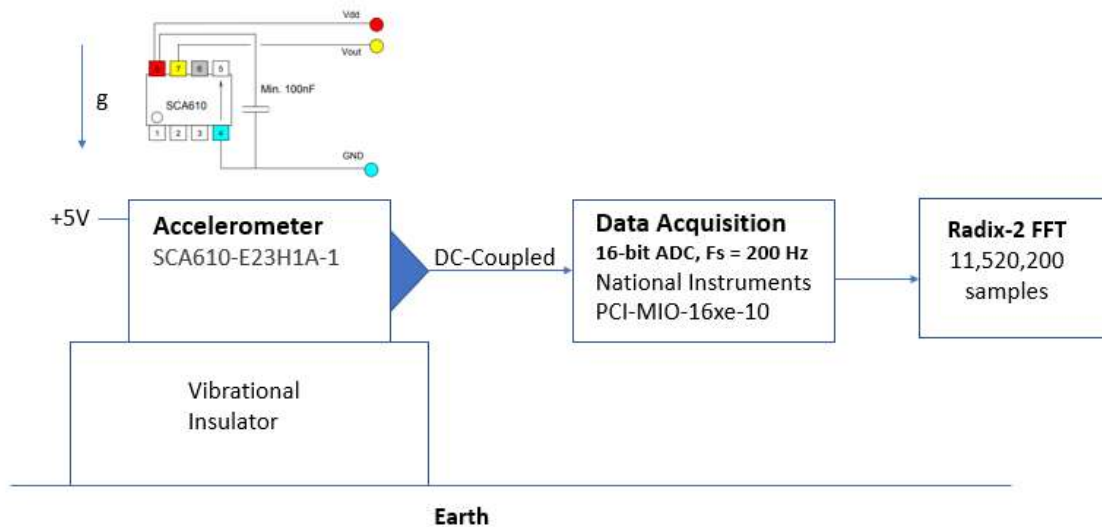

Figure 4a. Accelerometer Measurement Setup - Schematic

Figure 4b. Accelerometer Measurement Setup - Visual

The output from the accelerometer drives a National Instruments Data Acquisition board with a 16-bit ADC and a sampling rate of 200 Hz. Consequently, to 2x resolution on the lowest frequency of interest from (11) of $3.38 \; x \; 10^{-5} \; Hz$, approximately 11,520,200 samples are required at 200 Hz sample rate.

The first run of data was collected over a 16-hour period on Dec. 5th 2020, ending at 5:37:49 PM. An FFT was performed on the data producing the spectrum in Figure 5.
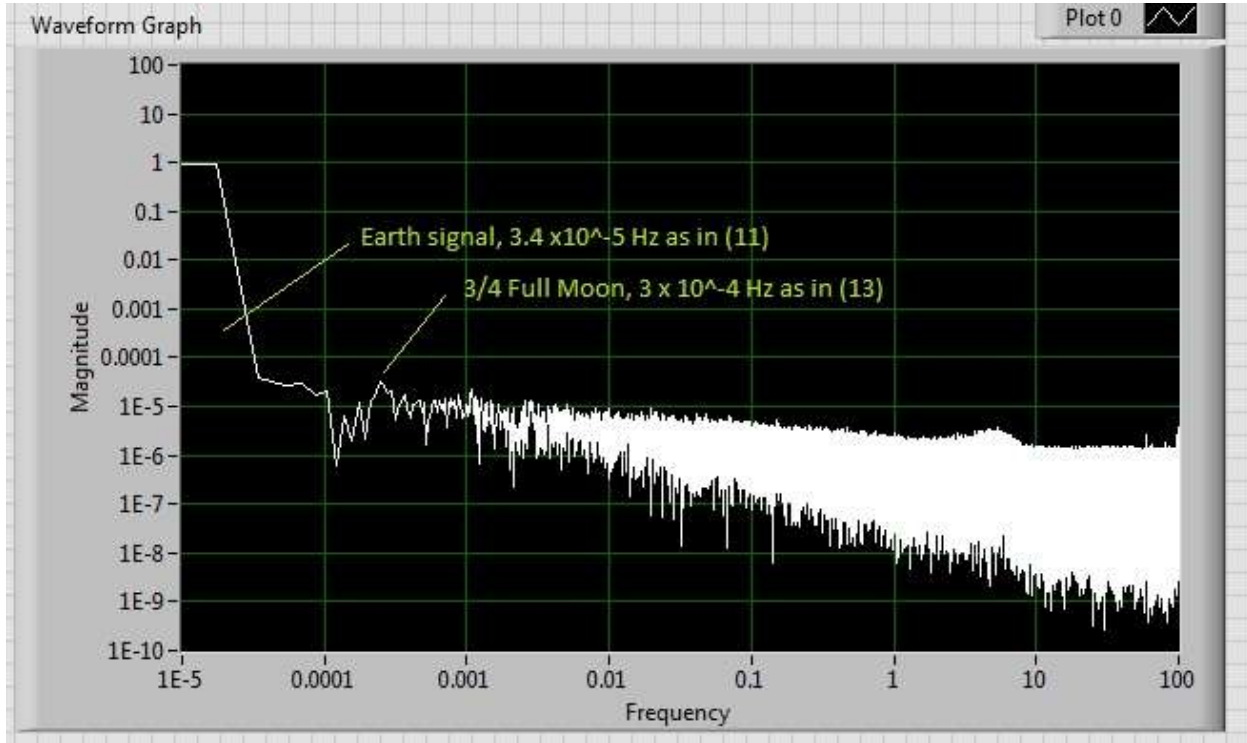

Figure 5. FFT of 16 Hour Run on Dec. 5th 2020 (Moon - Waning Gibbous)

As can be seen in Figure 5, the characteristic frequency of the Earth and Moon calculated respectively in (11) and (13) show peaks prior to dropping as smaller local masses dominate the nearby spectrum. We initially believed the time/frequency resolution for determining the characteristic frequency of the Earth was adequate, but after more consideration of the near-field characteristics of the Earth's spectrum detailed at the beginning of this section, we believe the frequency resolution in Fig. 5 to be too low of a resolution for measurement of Earth's signal and so all our future measurements are made at a higher-frequency resolution (which equates to 24-hour time runs or higher). The frequency resolution of the Moon's signal in Figure 5 is about 10x the Earth's frequency and is adequate for analysis however, and we notice that the ¾ full moon (Waning Gibbous) that occurred on Dec. 5th can be seen at a relative amplitude of 5 x 10^{-5} at the characteristic frequency of $3.05 \ x \ 10^{-4} \ Hz$ as predicted in (13).

As the analysis uses the mean distance values between the Earth and Moon, there can be significant variation in the amplitude of the Moon's signal based on its exact position relative to

the measurement location on Earth. Also, the location of the Moon relative to the Sun has an effect on the measurement of the Moon's gravitational wave signal. To demonstrate the higher resolution and show the Earth's signal more accurately as well as the effect of the Moon on the side of the Earth facing the Sun (a New Moon), Figure 6 details the results of a 32-hour run that was completed on Dec. 14th during the New Moon.
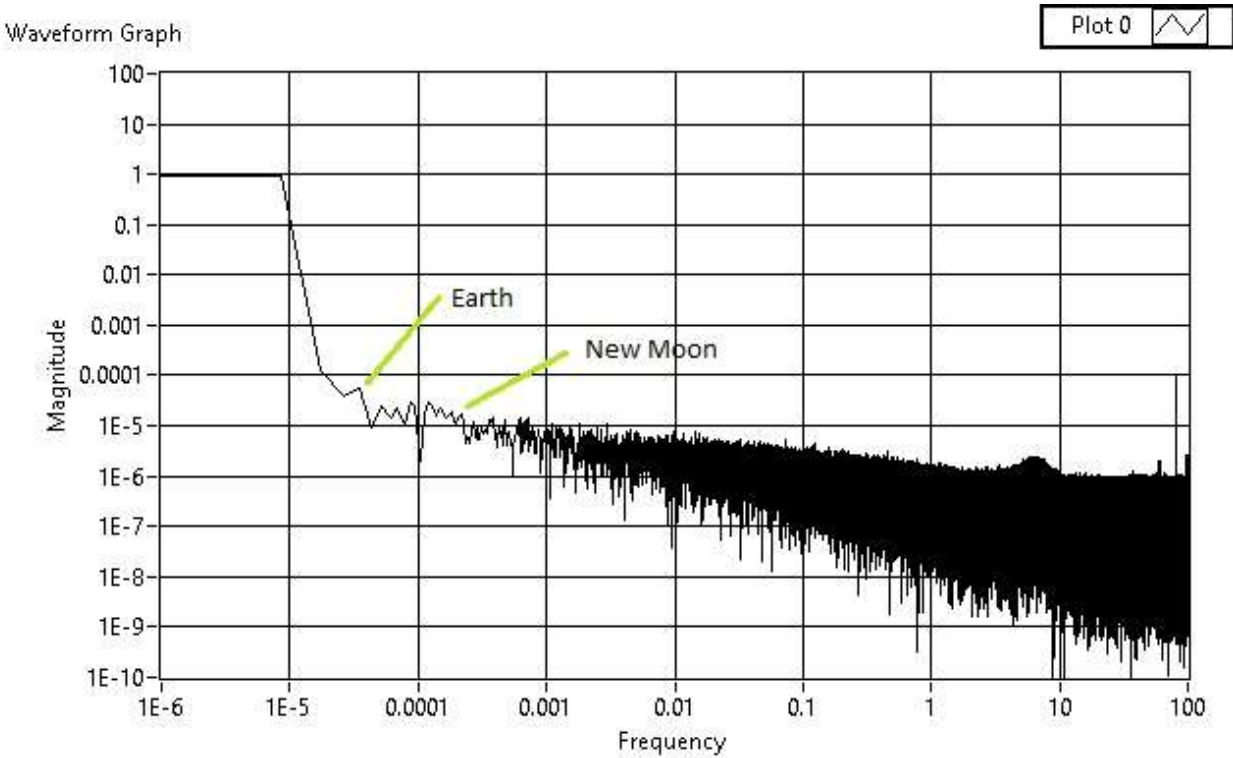

Figure 6. FFT of 32-Hour Run on Dec. 14th 2020 (New Moon)

Figure 6 shows the relative value of 8 x 10^-5 for the Earth's signal with a frequency peak at roughly 5 x 10^-5 Hz. Again, from an analysis at the beginning of this section, the near field measurement at the surface of the Earth is expected to be blurred by a wide-band of frequencies beginning at the characteristic frequency of $3.38 \; x \; 10^{-5}$ Hz and increasing in frequency as the high-frequency characteristic signals of electrons and protons broaden the near-field spectrum of the Earth's signal. It is worth noting that the New Moon signal can be seen at much lower amplitude than the ¾ Full Moon signal in Figure 5.

It is theorized that the New Moon, being in between the Earth and the stronger gravitational wave density (GWD) of the Sun, will produce a smaller signal in the background due to the

Sun's GWD interacting with the Earth. The Full Moon on the opposite side of the Earth is shielded from the Sun's GWD and therefore produces a relatively higher signal at the Earth's surface. This can be seen in Figure 7 for the ¾ Full Moon (Waxing Gibbous) run taken on Dec. 26, 2020.
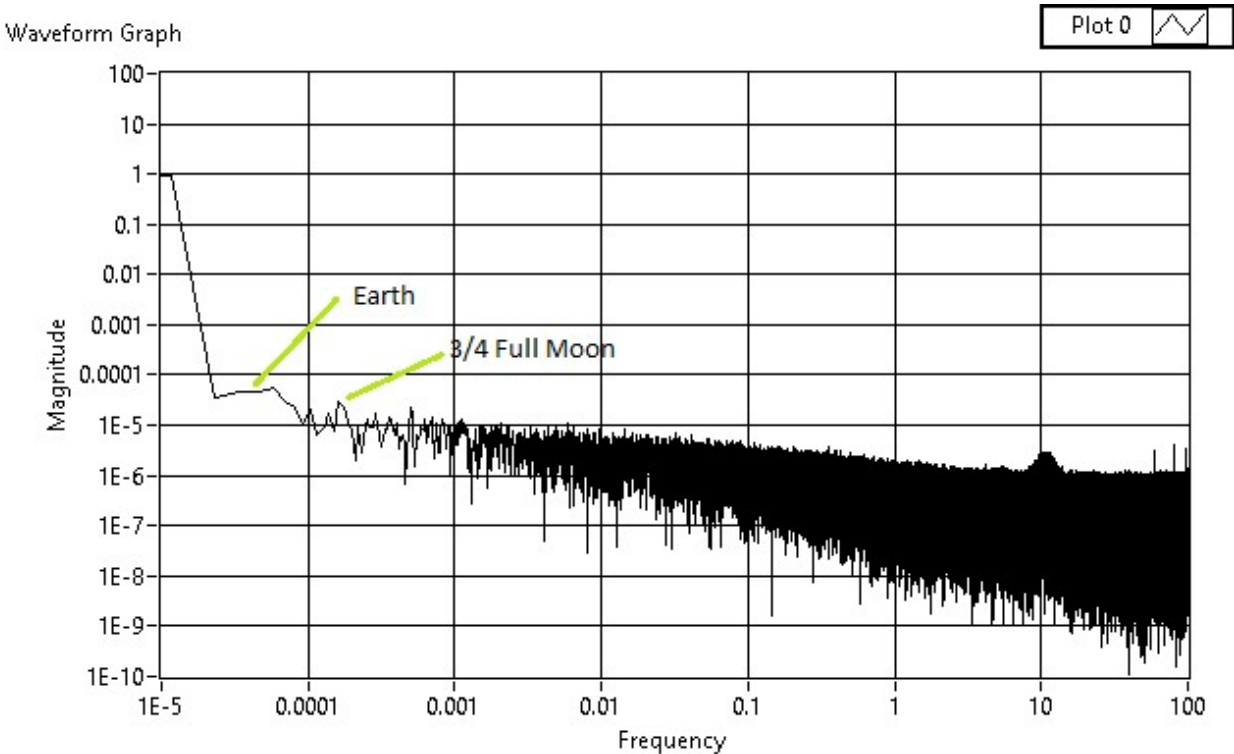
Figure 7. FFT of 24-Hour Run on Dec. 26th 2020 (Moon - Waxing Gibbous)

As can be seen in Figure 7, the Moon signal's amplitude is similar to the relative value of 5 x 10^{-5} shown in Figure 5 for the Waning Gibbous Moon on Dec. 5th. This is to be expected as the Moon is at the same relative angle to the horizon in both cases (just on opposite sides of the Earth producing Waning versus Waxing effect) and therefore results in similar amplitude measurements. The 24-hour run in Figure 7 shows the Earth's peak as a broader spectrum, indicating future measurements require 32 hours or more for detailed resolution as shown in Figure 6.

Figure 8 shows a 32-hour run starting on Dec. 28th at 8pm and running until Dec. 30th at 4am, which centers the run around the peak Full Moon of Dec. 29th, 2020.
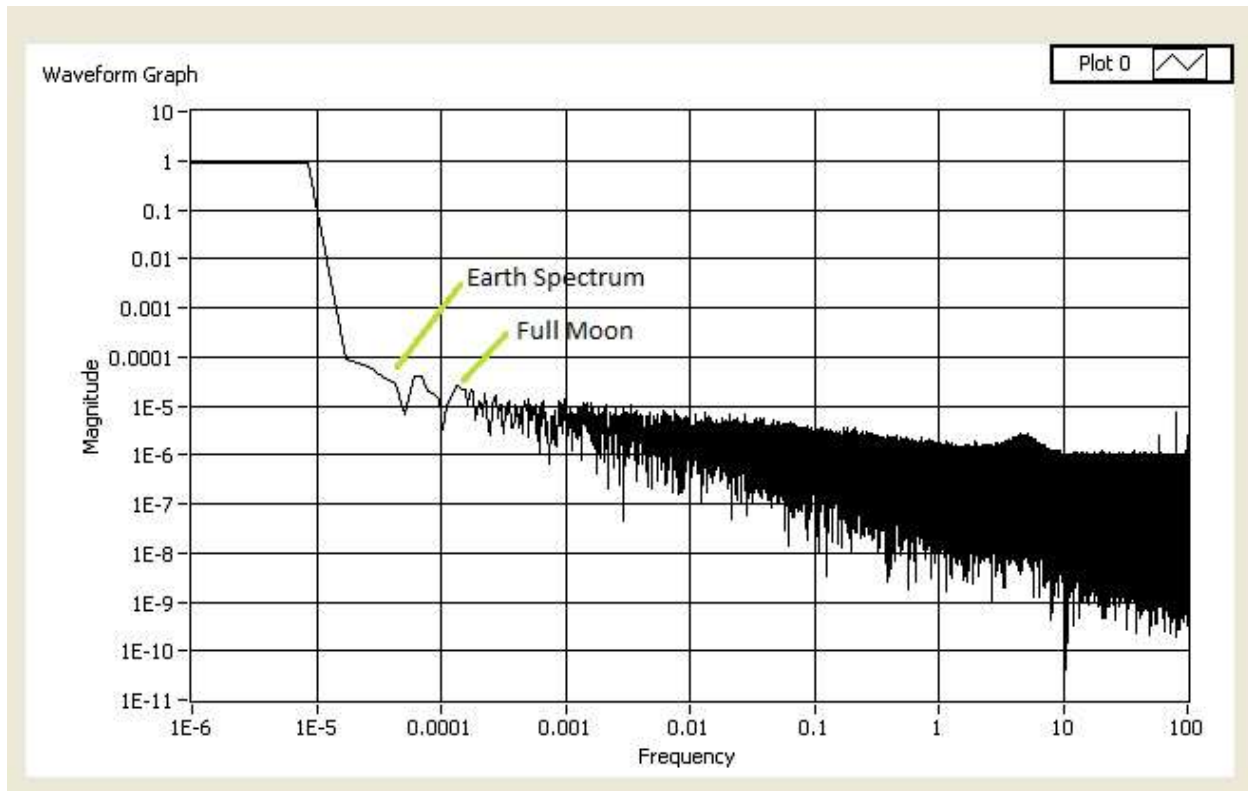
Figure 8. FFT of 32-Hour Run Centered Around Dec. 29ᵗʰ 2020 (Full Moon)

From Figure 8, we can see the similar peak of the Full Moon signal as in Fig 7 (Dec. 26) but with a broader spectrum, perhaps due to the higher frequency resolution of the 32-hour run time. The significant increase of the signal and distinctness of the peak around 3×10^{-4} Hz due to the Full Moon and ¾ Full Moon (Figures 8 and 7 respectively) are obviously more prominent than when compared with the more diffuse signal of the New Moon in Figure 6.

Continuous tracking of the Earth and Moon signals may reveal inter-modulations between the near-field of the Earth signal and mostly far-field of the Moon signal. This would result in sum and difference frequencies in the detector (our accelerometer in this case) that would produce slight variations in the frequency locations of the original signals.

VII.   Conclusions

The Wave Structure of Matter demonstrates that matter is composed of a dual wave structure, with incoming and outgoing waves of a modified Yukawa potential producing the effects we see as a point particle. The G44 solution of the field equations are reproduced with this model. With the calculation of the characteristic frequencies and relative amplitudes of the static gravitational waves from the Earth and Moon, we then perform an experiment to verify the results using a high-resolution MEMS accelerometer over a period of 30 days and we show the periodicity of the Moon signal during this time, with Full Moon resulting in a higher and broader peak as opposed to a diffuse signal during New Moon. Additional experiments are possible for tracking less massive objects in the higher-frequency spectrum as well as the potential for tracking near-Earth objects.

Acknowledgements

References

1. Hawking, S. W.; Israel, W. (1979). *General Relativity: An Einstein Centenary Survey*. Cambridge: Cambridge University Press. p. 98. *ISBN* *978-0-521-22285-3*.

2. Yukawa Potentials, https://en.wikipedia.org/wiki/Yukawa_potential

3. Wolff, Milo, "Exploring the Physics of the Unknown Universe: An Adventurer's Guide", Jan. 1, 1991, https://www.amazon.com/Exploring-Physics-Universe-Adventurers-Guide/dp/0962778702

4. Harney, Michael, "The Derivation of the Schwarzchild Solution from a Scalar Model of Spherical Quantum Waves", https://vixra.org/abs/1109.0008

5. http://physics.bu.edu/~redner/211-sp06/class01/MKS.html

6. Harney, Michael , "The Cosmological-Redshift Explained by the Intersection of Hubble Spheres", http://redshift.vif.com/JournalFiles/V13NO2PDF/V13N2HAR.pdf

7. LIGO, https://en.wikipedia.org/wiki/LIGO